

Cardiac neoplasms and pseudotumors: imaging findings on multidetector CT angiography

Edward Hoey, Arul Ganeshan, Kurdow Nader, Kiran Randhawa, Richard Watkin

ABSTRACT

A wide spectrum of masses can affect the heart, ranging from non-malignant entities, such as thrombi, to aggressive primary cardiac tumors, such as angiosarcomas. Echocardiography and magnetic resonance imaging have traditionally formed the mainstay techniques for assessing these lesions. Recent technological advances have seen ECG-gated multi-detector computed tomography (MDCT) emerge as a valuable complementary technique for assessing a suspected cardiac mass because it provides high spatial resolution, fast acquisition times, and the ability to definitively characterize fat and calcification. This article reviews the MDCT features of the spectrum of cardiac neoplasms and pseudotumors and describes important diagnostic criteria.

Key words: • computed tomography • angiography • neoplasms • heart

Cardiac masses are uncommon entities that can be broadly classified as non-neoplastic or neoplastic. Some normal anatomical structures (such as a prominent crista terminalis) and some non-neoplastic lesions (such as intracavitary thrombi) can mimic a true cardiac neoplasm.

Neoplastic masses are subdivided into metastatic, primary benign and primary malignant tumors. Because most cardiac masses are not amenable to biopsy, non-invasive imaging plays a pivotal role in their evaluation; imaging is also important if surgical resection is contemplated because accurate delineation of a lesion's margins helps predict the likelihood of complete removal (1).

A multi-modality imaging approach is usually required when investigating a suspected cardiac mass, with the choice of imaging technique guided by patient-related factors, local availability, and provider expertise. The primary goals of imaging are the following:

- 1) to ascertain if a mass is present;
- 2) to define a mass's location, extent, and relationships; and
- 3) to distinguish between potentially benign and malignant lesions.

Transthoracic echocardiography (TTE) is usually the initial imaging technique and is robust for identifying an intracardiac mass, provided that the acoustic windows are adequate. In patients with a large body habitus or emphysema, the evaluation is frequently limited. Transesophageal echocardiography (TEE) affords improved spatial resolution, which is especially useful for small masses (<1 cm) and valvular lesions. However, it is invasive and, as with TTE, provides only limited tissue characterization, often making it impossible to confidently distinguish between thrombi and benign and malignant tumors (1).

In recent years, magnetic resonance imaging (MRI) has become the technique of choice for further differentiation and characterization of a cardiac mass because it has numerous advantages over echocardiography, including an unrestricted field of view and superior soft-tissue resolution (2). However, MRI is heavily reliant on patient cooperation to obtain high quality images and is not suitable for all patients. It is specifically contraindicated in those patients with claustrophobia or an implanted ferromagnetic device.

Recent technologic advances in multi-detector computed tomography (MDCT), including improvements in spatial and temporal resolution in conjunction with ECG-gating, have made MDCT an extremely useful modality for evaluating a cardiac mass (3). ECG-gated MDCT should also be considered Superior to MRI in some respects as it has superior spatial resolution (0.4–0.6 mm vs. 1–2 mm), can definitively characterize fat and calcification using attenuation measurements and can simultaneously evaluate the coronary arteries.

From the Departments of Cardiovascular Radiology (E.H.✉ edwardhoey1@googlemail.com, A.G., K.N., K.R.) and Cardiology (R.W.), Heart of England NHS Trust, Birmingham, West Midlands, United Kingdom.

Received 12 January 2011; revision requested 14 February 2011; revision received 6 May 2011; accepted 7 May 2011.

Published online 1 November 2011
DOI 10.4261/1305-3825.DIR.4215-11.2

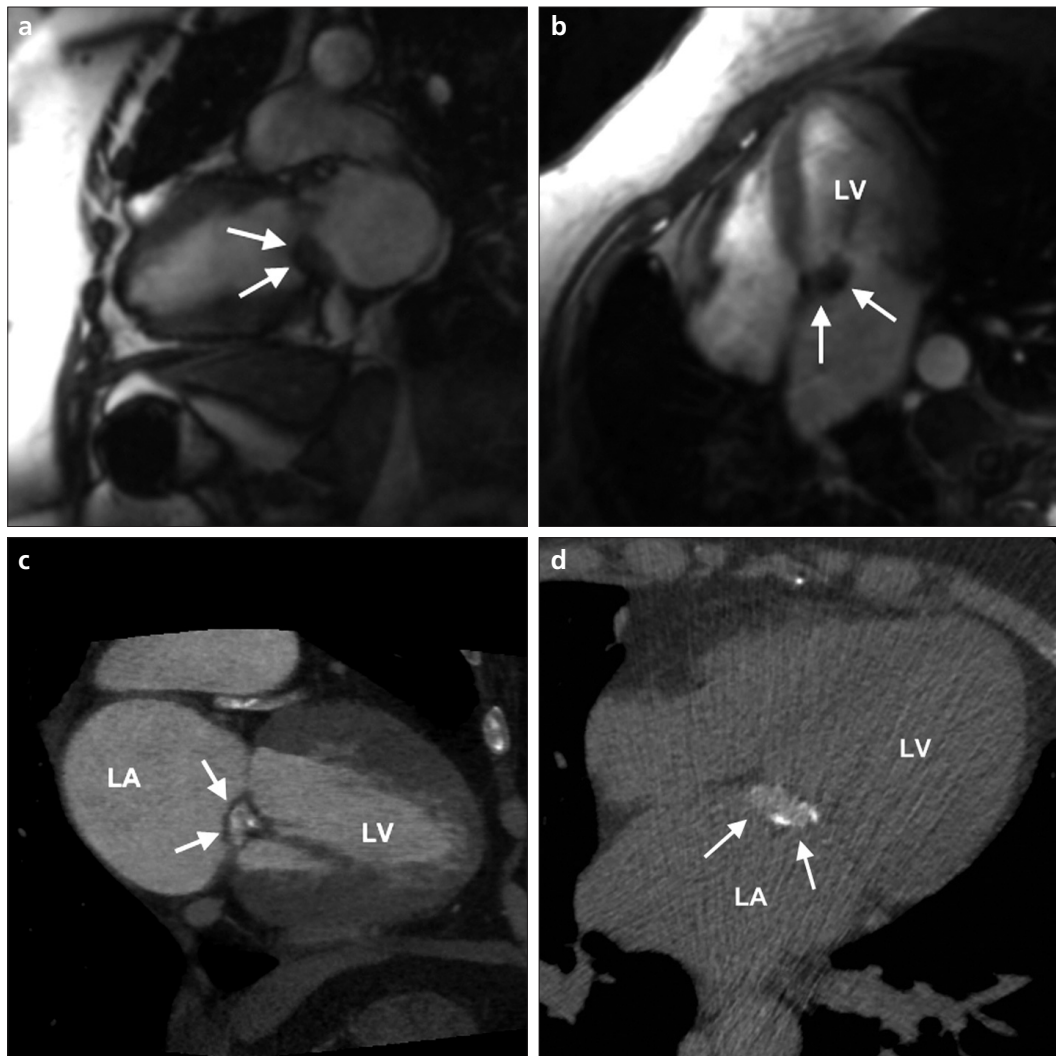


Figure 1. **a-d.** A suspected mass located near the mitral valve. MDCT was able to provide definitive assessment in this case, following an incomplete transthoracic echocardiogram (with limited acoustic windows) and inconclusive MRI study. A two-chamber SSFP MRI image (a) showing focal thickening of the anterior mitral valve leaflet (arrows). A four-chamber delayed-enhancement MRI image (b) acquired 10 minutes after injecting 0.1 mmol/kg gadolinium-DTPA and using an inversion recovery pulse sequence to attenuate the signal from the normal myocardium, showing absence of late enhancement (arrows). A two-chamber image from arterial phase ECG-gated MDCT (c). The improved spatial resolution of MDCT compared with MRI shows that the anterior mitral valve leaflet is "split" (arrows). This lesion is therefore a diverticulum rather than a "mass", as was suspected on the basis of the MRI. Also note the thickening and calcification of the sub-valvular apparatus, which is most likely secondary to rheumatic fever. A delayed-phase MDCT image (d) showing "trapping" of contrast medium within the diverticulum (arrows). LV, left ventricle; LA, left atrium.

Indeed, several consensus statements now include ECG-gated MDCT as a recommended technique for evaluating cardiac masses (4). Occasionally, a cardiac mass may be detected for the first time on non-ECG-gated thoracic MDCT studies performed for an unrelated indication, and radiologists should be familiar with its various characteristic features so that they can generate a meaningful differential diagnosis. This article describes the MDCT appearances of the most common cardiac pseudotumors and neoplasms.

Multidetector CT technique

To provide isotropic spatial resolution, MDCT studies are ideally performed using at least a 64-detector row system (3). Non-ECG gated MDCT with intravenous contrast infusion may be adequate for localizing a cardiac mass. In the absence of

ECG-gating, however, there are often significant motion artifacts, which can preclude detecting small lesions and cause blurring of the margins of larger lesions, thus limiting the assessment of local extension. ECG-gating minimizes cardiac motion-related artifacts, thus enabling more precise evaluation of lesion margins. Retrospective ECG-gating (continuous data acquisition through the cardiac cycle) is preferred over prospective ECG-gating (data acquisition at a single time point) because it allows cine loops to be reconstructed, and lesion mobility can be assessed. Retrospective ECG-gating carries a much higher radiation burden than prospective ECG-gating (10–15 mSv vs. 2–5 mSv), however. Scanning from the carina to the cardiac apex usually provides a sufficient volume of coverage. We typically use 70 mL of iodinated contrast medium at 5 mL/s followed by a

50%:50% contrast:saline flush, which helps maintain some opacification in the right heart chambers but which is not so dense as to create streak artifacts. A follow-up study 2–3 min later without additional contrast injection can help with tissue characterization because delayed enhancement within a mass signifies contrast accumulation in an expanded interstitium, such as within areas of tumor necrosis. Delayed phase images may also be a useful problem-solving technique in cases where evaluations with echocardiography and/or MRI have been incomplete or inconclusive (Fig. 1). Prospective ECG-gating with a low tube voltage (80 kV) and normal tube current (600–800 mAs) has been recommended to minimize radiation exposure while maximizing the contrast-to-noise ratio between the tumor tissue and normal myocardium in delayed phase MDCT (5).

The images are reconstructed with a 0.75-mm slice thickness and read on a viewing platform with multi-planar capabilities. The images are initially reviewed in the axial plane and then reconstructed in the standard cardiac imaging planes: vertical long axis (two-chamber), horizontal long axis (four-chamber), left ventricular short axis, and left ventricular outflow tract (three-chamber).

Pseudotumors

A variety of non-neoplastic masses can mimic cardiac tumors and should be recognized as such to avoid misdiagnosis.

Intracavitory thrombi

Thrombi are the most common intracardiac masses and are the major differential for any intracavitory lesion. Most thrombi develop in regions of slow flow or around a nidus, such as a central venous catheter tip. Common locations for a thrombus are the left ventricle, in association with aneurysm formation after myocardial infarctions, and the left atrial appendage, in patients with atrial fibrillation (Fig. 2). On MDCT, a thrombus appears as a well-circumscribed, low-attenuation mass that usually does not enhance, even on delayed phase scans. Rarely, chronic thrombi may show some peripheral enhancement due to the presence of a fibrous pseudocapsule (Fig. 3). Chronic thrombi may occasionally contain calcifications. The main differential is atrial myxoma, for which there can be considerable overlap of MDCT imaging results. Indeed, a recent study by Scheffel et al. (6) showed that prolapse through the atrioventricular valve orifice is the only reliable feature favoring myxoma over left atrial thrombus on ECG-gated MDCT; lesion size, origin, and attenuation characteristics were poor discriminators.

Lipomatous hypertrophy

Lipomatous hypertrophy of the atrial septum describes an excess of normal brown fat in this region and is considered an anatomical variant rather than a true neoplasm. Unlike an interatrial lipoma, which is the main differential diagnosis, it characteristically spares the fossa ovalis, which gives it a dumbbell-like appearance (Fig. 4) (7).

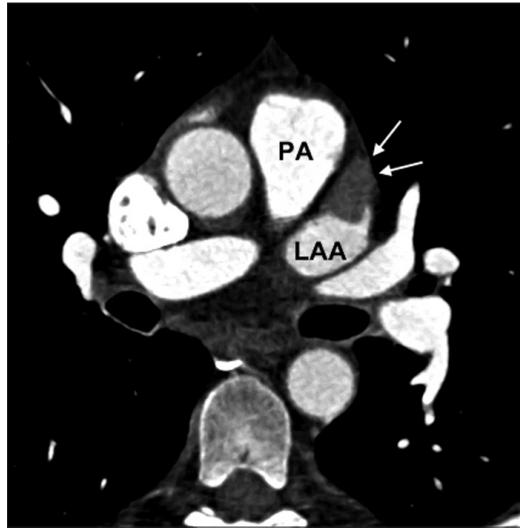


Figure 2. A left atrial appendage thrombus in a patient with atrial fibrillation. This ECG-gated axial arterial phase MDCT image shows a low attenuation-filling defect within the left atrial appendage (arrows). PA, pulmonary artery; LAA, left atrial appendage.



Figure 3. a, b. A left ventricular thrombus in a patient with ischemic cardiomyopathy. A non-ECG-gated axial arterial phase MDCT image (a) showing a subtle laminated thrombus adherent to the interventricular septum (arrows). The left ventricle is dilated, and there are signs of decompensation with bilateral pleural effusions (asterisks). A delayed phase image (b) showing non-enhancement of the thrombus compared with the adjacent myocardium, which makes it more conspicuous (arrows). RV, right ventricle.

Normal anatomical structures

The crista terminalis is a vertically orientated fibromuscular ridge that runs along the posterior wall of the right atrium; its size and shape may

vary considerably among individuals. The moderator band extends obliquely across the right ventricle, contains conduction fibers, and should not be mistaken for a mass (3).

Pericardial cyst

Pericardial cysts are benign congenital lesions that arise from the pericardium but do not communicate with the pericardial space. They have an incidence of 1:100 000 and are most commonly located at the right anterior cardiophrenic angle, although they may occur anywhere in the mediastinum (8). They are simple unilocular lesions that contain water-based fluid without internal septa. Although usually asymptomatic, some patients may complain of symptoms that include chest pain and persistent cough. MDCT shows a homogenous, non-enhancing mass of water attenuation (Fig. 5).

Bronchogenic cyst

Bronchogenic cysts are well-circumscribed, thin-walled, fluid-filled structures that are thought to arise from the bronchial tree as a result of abnormal budding of the ventral foregut. Approximately two-thirds are situated within the mediastinum, most often in a subcarinal or right paratracheal location. MDCT shows a sharply marginated mediastinal mass consisting of soft-tissue or water attenuation.

Pericardial hematoma

Pericardial hematomas usually result from prior cardiac surgery, trauma or myocardial infarction. In an acute context, compression of the cardiac chambers may impede diastolic ventricular filling and lead to hemodynamic compromise. Chronic hematomas tend to become organized, often calcify, and are a frequent cause of constrictive pericarditis. Calcification is manifest as a signal void on all MRI pulse sequences, and MDCT is the modality of choice for a definitive characterization (Fig. 6).

Metastases

Metastases to the heart and pericardium are 100–1000 times more common than primary cardiac tumors (9). They generally appear late in the course of the primary disease, and isolated cardiac involvement is rare in the absence of multi-organ dissemination. The spreading mechanisms include direct extension (Fig. 7) and hematogenous and venous seeding (Fig. 8), with hematogenous seeding being the most common route



Figure 4. Lipomatous hypertrophy of the atrial septum, which was an incidental finding on a non-ECG-gated thoracic MDCT. An axial image showing the classical uniform fat attenuation (-100 HU) and "dumbbell" thickening of the atrial septum (arrows), which spares the mid-septum (fossa ovalis). LV, left ventricle.

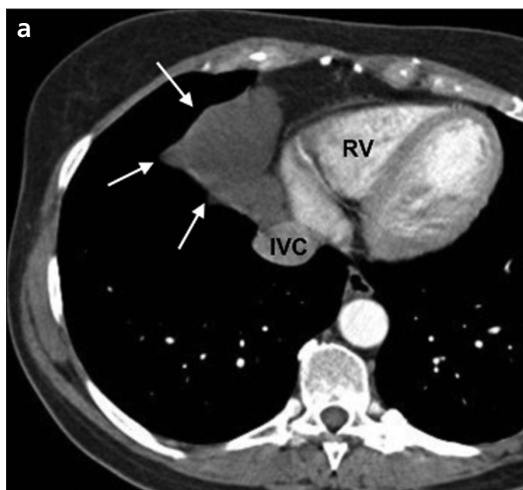
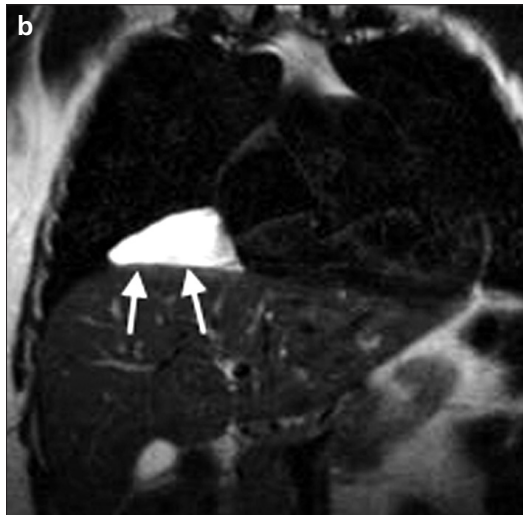


Figure 5. a, b. A pericardial cyst that was an incidental finding. An axial MDCT image (a) showing a well-circumscribed and uniformly low-attenuation structure in the right cardiophrenic angle (arrows). A coronal T2-weighted MR image (b) showing uniform high signal within the lesion (arrows), confirming its fluid content. RV, right ventricle; IVC, inferior vena cava.



for tumors of bronchial and breast origin (the majority of the primary lesions). The pericardium is the most frequent site of involvement, which often takes the form of a malignant

effusion. Aside from pericardial effusions, metastases may also manifest on MDCT as multiple soft-tissue density masses (9).

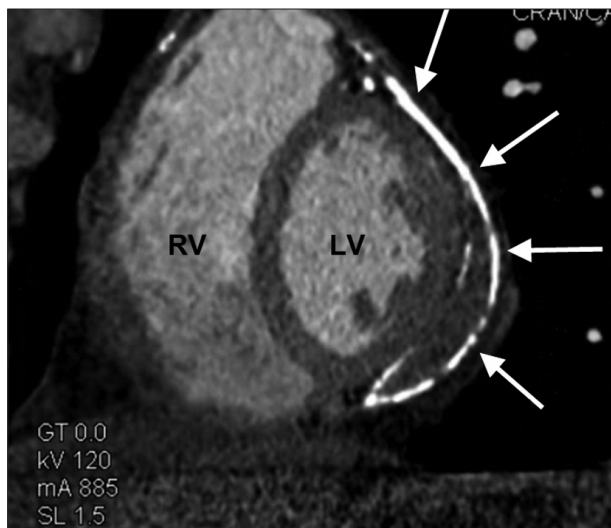


Figure 6. Constrictive pericarditis secondary to a calcified pericardial hematoma. This short-axis, arterial-phase ECG-gated MDCT image at the level of the mid portion of the left ventricle shows heavy pericardial calcification (arrows). There is indentation of the left ventricle, suggesting a degree of hemodynamic compromise. RV, right ventricle; LV, left ventricle.

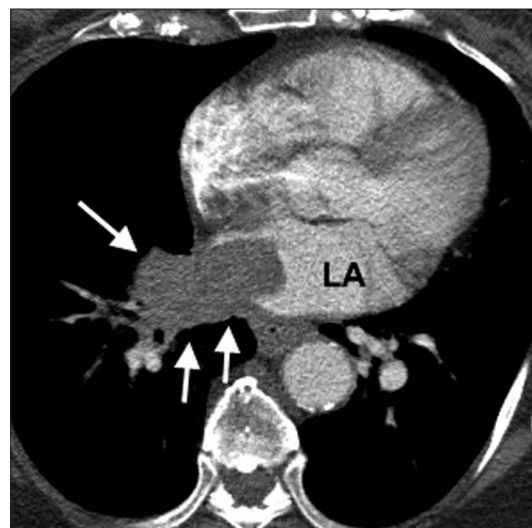


Figure 7. The direct extension of a bronchogenic carcinoma into the left atrium. This axial MDCT image shows a tumor extending along the right inferior pulmonary vein (arrows). LA, left atrium.

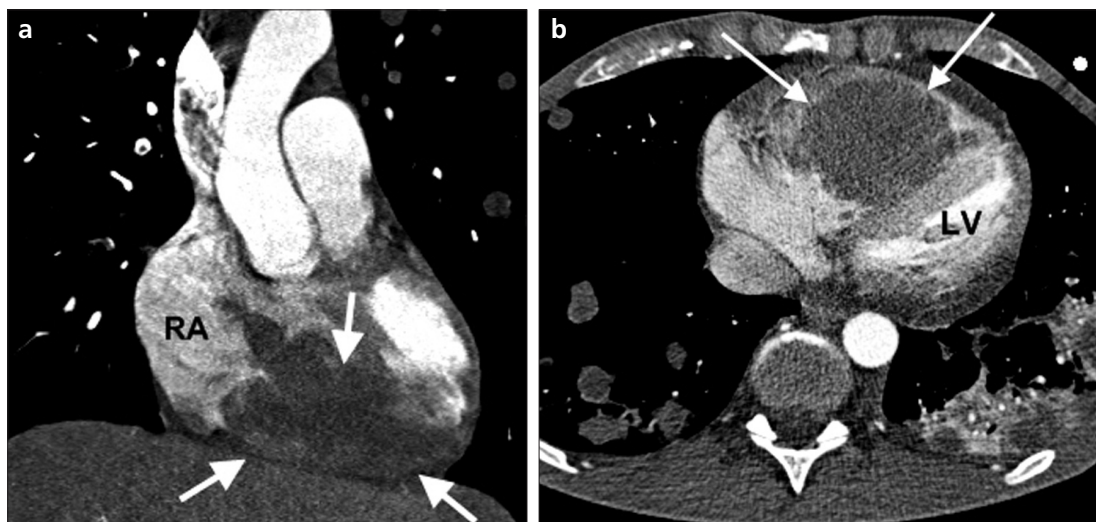


Figure 8. a, b. The hematogenous spread of metastases from an advanced testicular tumor, as depicted by a non-ECG-gated MDCT study. A coronal image (a) showing large deposits filling and expanding into the right ventricle (arrows). Also note several left lung nodules. An axial image (b) showing multiple deposits lodged within the proximal pulmonary arteries and multiple parenchymal nodules (arrows). RA, right atrium; LV, left ventricle.

Primary cardiac tumors

Primary cardiac tumors are rare, with an estimated lifetime incidence of 0.02% (10). The approximate frequencies of the subtypes, taken from the surgical and pathology literature, are presented in Table. The clinical manifestations are non-specific and depend on size, tumor type, and location. While some remain clinically silent, others present with symptoms, such as intracardiac obstruction, tamponade,

arrhythmias, and systemic embolization (11).

Benign primary tumors

Most benign primary cardiac tumors can be completely resected with minimal morbidity and mortality, and many patients enjoy survival similar to that of the general population (10). The typical features include a well-defined mass that involves a single cardiac chamber and has a narrow transition zone.

Myxoma

Myxomas account for 50% of all benign primary cardiac tumors and may arise from pluripotent residual mesenchymal cells in the subendocardium (11). The vast majority arise within the atria, with 75% occurring on the left and 15%–20% on the right side. A narrow attachment point at the fossa ovalis of the atrial septum is typical, but they can originate from any endocardial surface, including the valves (1).

Resection is required for definitive diagnosis and to prevent major complications, especially strokes secondary to the systemic embolization of left-sided tumor fragments (1).

Most myxomas appear on MDCT as pedunculated low-attenuation intracavitory masses (Fig. 9), although some myxomas are broad based and contain calcifications. Large lesions may prolapse through the mitral or tricuspid valve orifices (Fig. 10) (6). Arterial phase enhancement is usually not apparent, but delayed enhancement is recognized and typically heterogeneous (6). Thrombus is the major differential diagnosis, as has been previously discussed.

Fibroelastoma

Fibroelastomas are endocardial papillomas composed of collagen and elastic-tissue fibers, with an endothelial covering and a connective tissue pedicle. They can arise from any endocardial surface, but the majority are found on the aortic and mitral valves (12). Most are small (<1 cm) and remain clinically silent, but there is the potential for embolization into the systemic or pulmonary circulation from accumulated thrombi.

Because of their small size, TEE is the optimal means of detection, and MDCT assessment is rarely indicated; however, they are occasional findings on MDCT appearing as a focal low attenuation valve nodule (3). Fibroelastomas are typically located away from the valvular free edge, and the valve function is usually preserved; this outcome is in contrast to endocarditis-induced vegetation, which also appears as a low attenuation lesion but which typically involves the valvular free edge and causes valve destruction and dysfunction (1). In our experience, we have found multi-sequence MRI more useful than MDCT in the pre-operative work-up of suspected fibroelastomas (Fig. 11).

Lipoma

Lipomas are slow growing neoplasms composed of mature adipose tissue. They may arise from the epicardial, myocardial or endocardial surfaces, including the atrial septum (7). Most patients are asymptomatic, but these tumors are a recognized cause of arrhythmias, especially atrial fibrillation. Large lipomas can sometimes produce

Table. The approximate frequency of benign and malignant primary cardiac tumors, adapted from references 10 and 11

	Percentage
Benign	
Myxoma	50%
Fibroelastoma	15%
Lipoma	5%
Fibroma	4%
Other	1%
Total	75%
Malignant	
Angiosarcoma	10%
Sarcomas with myofibroblastic differentiation	
Undifferentiated pleomorphic sarcoma	5%
Osteosarcoma	1%
Leiomyosarcoma	<1%
Fibrosarcoma	<1%
Liposarcoma	<1%
Myofibroblastic tumor	<1%
Rhabdomyosarcoma	5%
Primary lymphoma	1%
Pericardial tumor	
Mesothelioma	2%
Synovial sarcoma	<1%
Total	25%

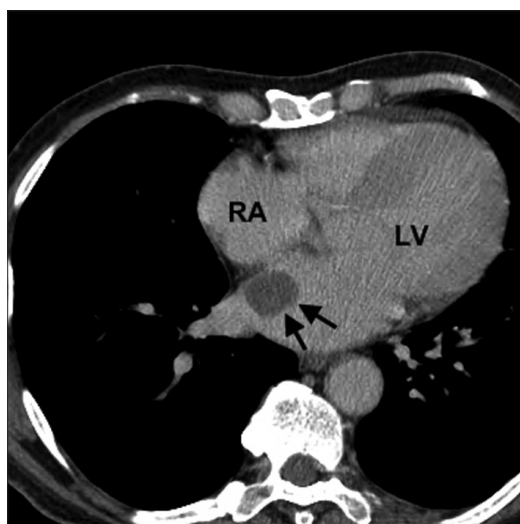


Figure 9. A small left atrial myxoma, which was an incidental finding. This axial MDCT image shows a well-circumscribed, low-attenuation mass in relation to the atrial septum (arrows). A thrombus can have an identical CT appearance; however, this lesion failed to resolve with anticoagulation and was subsequently surgically resected, which confirmed the diagnosis of myxoma. RA, right atrium; LV, left ventricle.

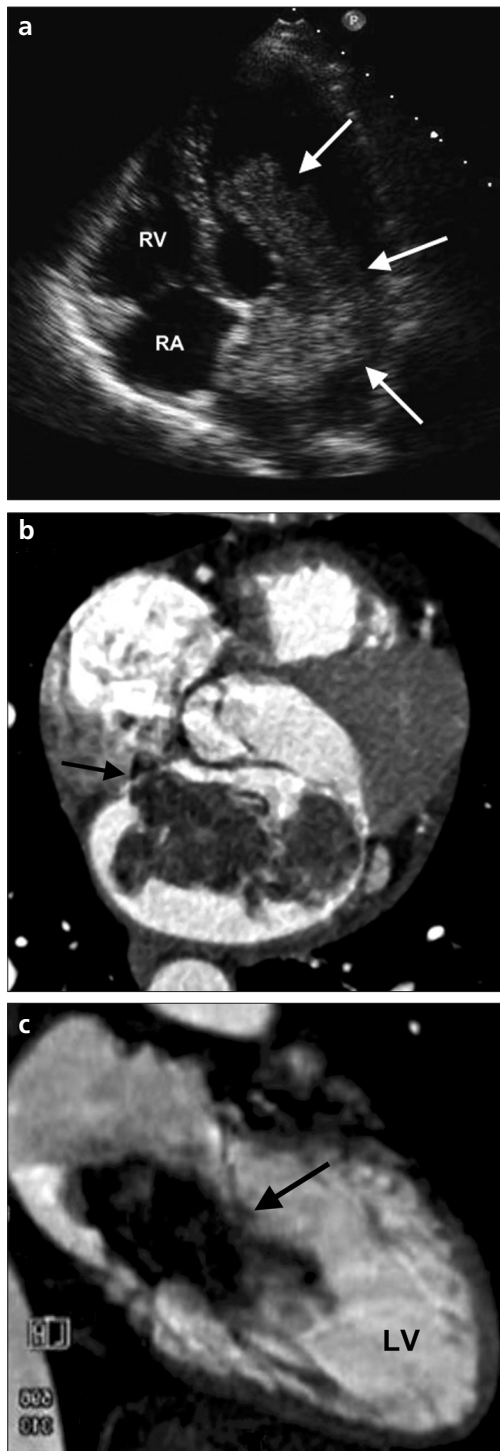


Figure 10. a–c. A large left atrial myxoma in a patient who presented with palpitations and embolic phenomena. A diastolic phase echocardiogram image (a) showing a large mass prolapsing through the mitral valve orifice (arrows). An axial ECG-gated MDCT image (b) showing that the lesion is attached to the atrial septum by a narrow pedicle (arrow) and has low attenuation and a villous margin. A two-chamber MDCT image (c) in diastole showing lesion prolapse through the mitral valve orifice (arrow), which is considered a reliable means of distinguishing myxomas from thrombi. RA, right atrium; RV, right ventricle; LV, left ventricle.

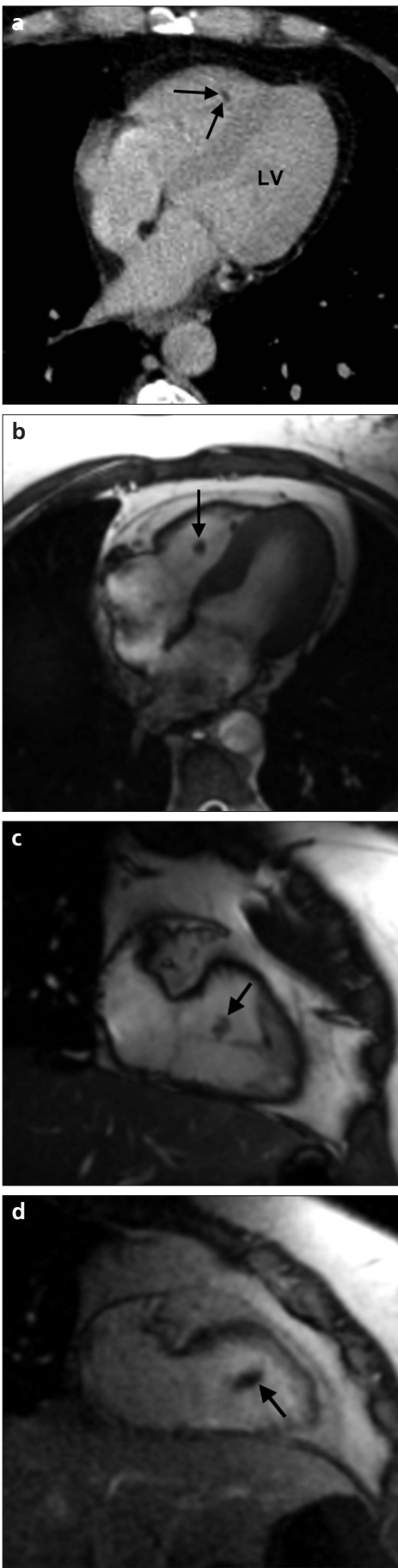


Figure 11. a–d. A fibroelastoma of the tricuspid valve, which was an incidental finding in a contrast-enhanced thoracic MDCT study performed for a different indication. An MRI was performed for further characterization, and the findings were typical for a papillary fibroelastoma. An axial non-ECG-gated MDCT image (a) showing a tiny, well-circumscribed low-attenuation nodule within the right ventricular cavity (arrows). A four-chamber SSFP MRI image (b) and a coronal SSFP MRI image (c) showing that the nodule is attached to the tricuspid sub-valvular apparatus (arrows). A delayed gadolinium-enhanced image (d) acquired 10 min following the injection of 0.1 mmol/kg gadolinium-DTPA and using an inversion-recovery pulse sequence to attenuate the signal from the normal myocardium. It shows complete absence of enhancement within the nodule (arrow), which supports a benign etiology. The morphological information provided by the MRI is most consistent with papillary fibroelastoma. LV, left ventricle.

symptoms secondary to their compressive effects. Lipomas are difficult to diagnose using echocardiography due to an extremely variable echo-pattern (1). Both MRI and MDCT are reliable techniques for definitively characterizing fat. On MDCT, a lipoma appears as a well-circumscribed lesion of homogeneous fat attenuation (-50 to -150 HU) (Fig. 12).

Fibroma

Fibromas are well-circumscribed aggregates of collagen and fibroblasts that arise in an intra-myocardial location, most often in the ventricular septum or left-ventricular free wall. Although histologically benign, they can cause ventricular arrhythmias and sudden death from interference with conduction pathways (2, 11). The majority occur in infants and children, but presentation in adulthood also occurs. On MDCT, a fibroma appears as a discrete focal soft-tissue attenuation mass (Fig. 13) that sometimes contains foci of calcification (3).

Other benign tumors

Rhabdomyomas usually occur in association with tuberous sclerosis. They are common in childhood but tend to regress spontaneously and are rarely encountered in adults. On MDCT, they manifest as single or multiple solid homogeneous masses arising in the left ventricular myocardium (1).

Hemangiomas are vascular malformations composed of blood-filled, endothelial-lined, and thin-walled spaces. Most patients are asymptomatic, and they are often discovered incidentally at cardiac surgery, although exertional dyspnea is a recognized presentation. On MDCT, hemangiomas appear as well-defined expansile masses within the ventricular myocardium/pericardium and may contain calcifications; enhancement is usually avid and prolonged (3).

Paragangliomas originate from cardiac neuroendocrine cells, and patients typically present with symptoms of excess catecholamines, e.g., hypertension and flushing. Resection is usually curative provided it is complete. On MDCT, paragangliomas appear as discrete, heterogeneous low-attenuation masses in the typical cardiac ganglia distribution pathways, i.e., at the root of the great vessels and along the walls of the atria (2).



Figure 12. An interatrial lipoma in a patient with supraventricular tachycardia. A four-chamber image from an ECG-gated MDCT study showing a large well-circumscribed lesion (arrows) within the atrial septum that has uniform fat attenuation (-110 HU). LV, left ventricle; RV, right ventricle.

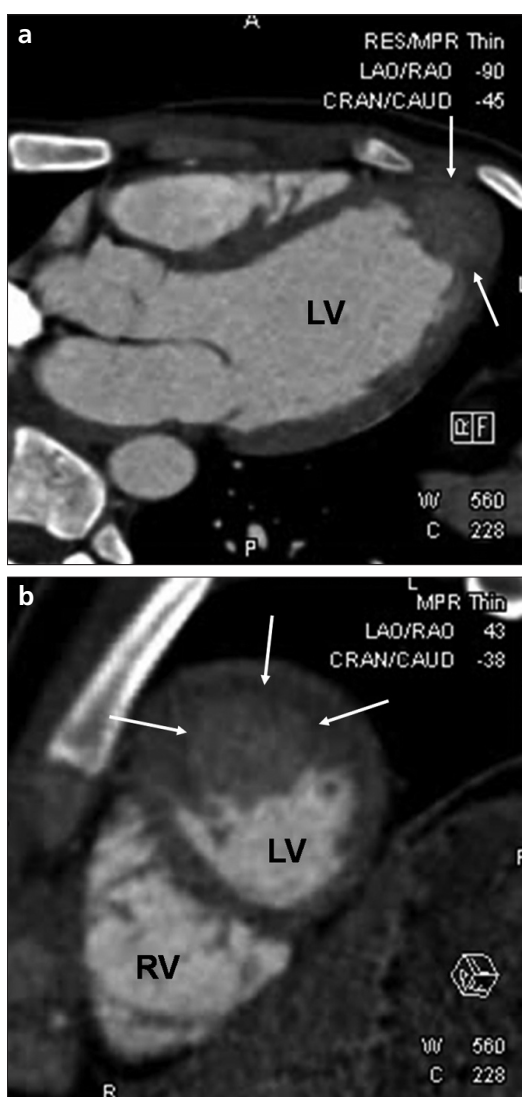


Figure 13. **a.** A fibroma of the left ventricle in a patient with palpitations. A three-chamber MDCT image (a) showing a well-circumscribed, soft-tissue attenuated intra-myocardial mass at the left ventricular apex (arrows). **b.** A short-axis MDCT image (b) that again shows the well-defined margins of this tumor (arrows). LV, left ventricle; RV, right ventricle.

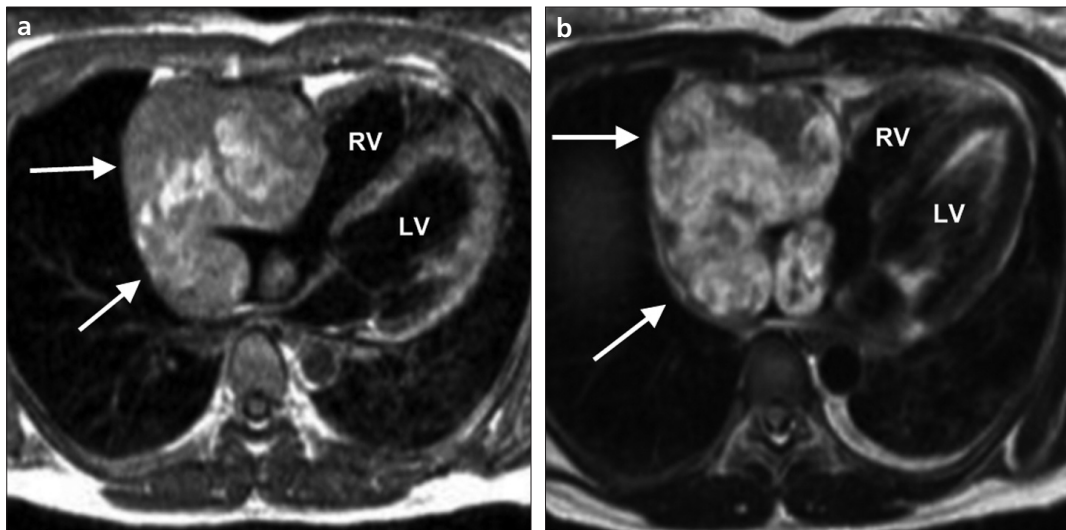


Figure 14. **a, b.** An angiosarcoma arising from the right atrial free wall in a patient with symptoms of right heart failure. An axial T1-weighted MR image (**a**) showing a large mass with mixed signal intensity centered on the right atrium (arrows). The central high signal areas may reflect hemorrhagic foci within this highly vascular lesion. An axial T2-weighted MR images (**b**) showing that the lesion has high water content (arrows), which is very suggestive of a malignant etiology. LV, left ventricle; RV, right ventricle.

Malignant primary tumors

Imaging findings suggestive of a malignant cardiac tumor include a right atrial location, involvement of more than one cardiac chamber, size >5 cm, hemorrhagic pericardial effusion, a broad base of attachment, extension into the mediastinum or great vessels, and delayed enhancement (13).

Sarcomas

Sarcomas account for the majority of primary malignant cardiac tumors and are the second most common primary tumor after myxomas. Histologically, they are classified into three main subgroups: angiosarcomas, sarcomas with myofibroblastic differentiation, and rhabdomyosarcomas (11).

Angiosarcomas

Angiosarcomas are highly aggressive neoplasms composed of irregular vascular channels lined by anaplastic epithelial cells. The peak incidence is in the fourth decade, and there is a strong male predominance. The majority originate in the right atrium; they typically fill this chamber, with infiltration along the pericardium and into the tricuspid valve and right coronary artery (1, 2). The clinical presentation usually occurs at an advanced stage, with symptoms of right heart failure and/or cardiac tamponade (11). Distant metastases are present in up to 90% of the cases at the time of diagnosis; these metastases most frequently

occur in the lungs, liver, and brain. The prognosis is dire, with few patients surviving beyond 12 months (14). MRI is the technique of choice for assessing the precise relationship of the tumor to adjacent structures if resection or debulking surgery is being contemplated (Fig. 14). On imaging studies, angiosarcomas typically appear as large masses with a heterogeneous composition, often in association with sheet-like pericardial thickening and a hemorrhagic pericardial effusion.

Sarcomas with myofibroblastic differentiation

This group of tumors is diverse and may contain heterologous elements, such as bone. They occur predominantly in adulthood and are sub-classified as undifferentiated sarcomas, leiomyosarcomas, fibrosarcomas, liposarcomas, and osteosarcomas. They most often originate along the posterior wall of the left atrium and tend to exhibit slow infiltrative growth patterns (3). Their infiltrative nature is readily appreciated on MDCT, which helps differentiate them from thrombi and myxoma (Fig. 15). Calcifications should alert physicians to the possibility of an osteosarcoma. Liposarcomas rarely contain sufficient amounts of macroscopic fat to permit confident diagnosis based on their morphologic imaging characteristics (2).

Rhabdomyosarcomas

Rhabdomyosarcomas are malignant tumors of striated muscle. Although they account for only around 5% of adult primary cardiac tumors, they are the most common pediatric cardiac malignancy. Rhabdomyosarcomas may arise anywhere in the myocardium, with a tendency towards multiple sites of origin, valvular involvement and extension into the pericardial space. On MDCT, they usually appear as a large infiltrative mass that may contain central areas of necrosis (Fig. 16). When the pericardium is involved, it usually has a nodular appearance; this finding is in contrast to angiosarcomas, which usually produce sheet-like thickening (1).

Primary cardiac lymphomas

Primary cardiac lymphoma describes a disease that is confined to the heart or pericardium, which distinguishes it from the more common case of cardiac involvement by non-Hodgkin's lymphoma (3). Most of these lymphomas occur in immunocompromised patients, are of B-cell origin, and follow an aggressive clinical course. Unlike other primary cardiac malignancies, they often have a favorable response to chemotherapy. The right atrium is reported to be the most common site, but unlike sarcomas, they are less likely to have necrosis and rarely involve the valves (1). The imaging findings are non-specific,

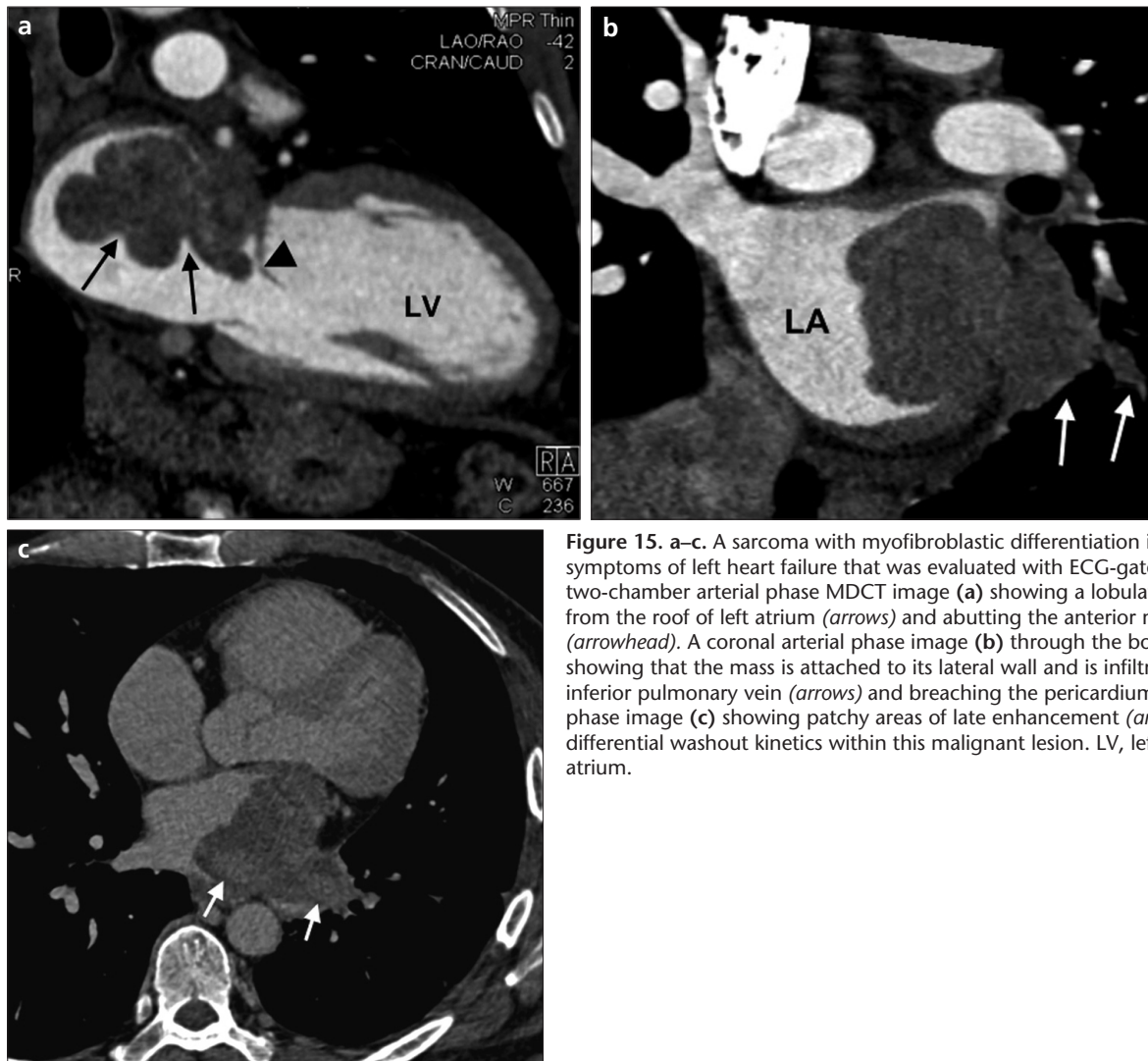


Figure 15. a–c. A sarcoma with myofibroblastic differentiation in a patient with symptoms of left heart failure that was evaluated with ECG-gated MDCT. A two-chamber arterial phase MDCT image (a) showing a lobulated mass arising from the roof of left atrium (arrows) and abutting the anterior mitral valve leaflet (arrowhead). A coronal arterial phase image (b) through the body of left atrium showing that the mass is attached to its lateral wall and is infiltrating into the left inferior pulmonary vein (arrows) and breaching the pericardium. An axial delayed-phase image (c) showing patchy areas of late enhancement (arrows), which implies differential washout kinetics within this malignant lesion. LV, left ventricle; LA, left atrium.

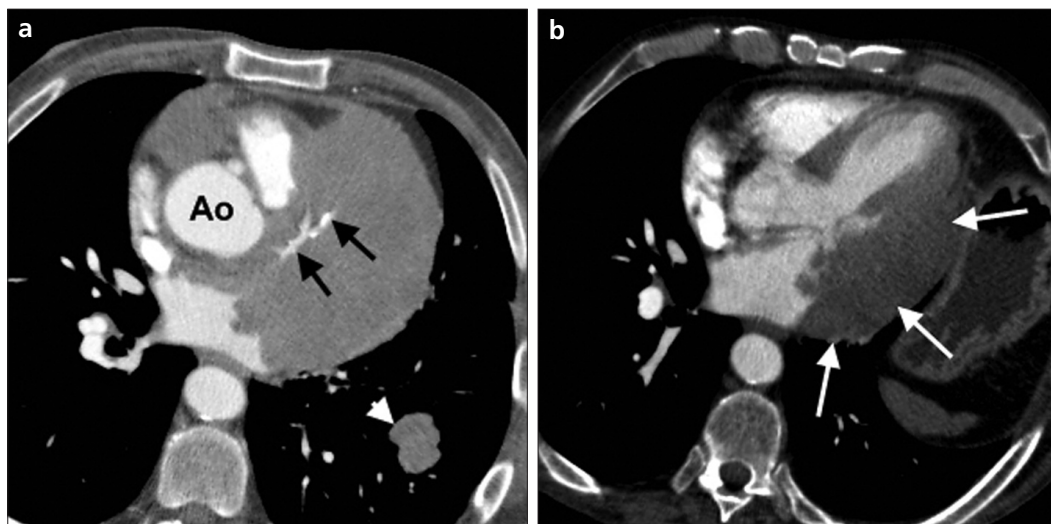


Figure 16. a, b. A rhabdomyosarcoma in a patient with chest pain and weight loss. An axial MDCT image (a) at the level of the aortic root showing tumor infiltration surrounding the left anterior descending coronary artery (arrows). Also note the presence of a pulmonary metastasis (arrowhead). Axial MDCT image (b) at the level of the left atrium shows a large infiltrative mass centered on the left ventricular free wall (arrows). Ao, aortic root.

but they usually appear as isoattenuating relative to myocardium on MDCT. Several morphologic subtypes have been described, including a solitary nodular mass and a diffuse infiltrative process, often in association with extensive pericardial effusion.

Primary pericardial malignancy

Mesothelioma can arise from the pericardial mesothelial cell layer. An association with asbestos exposure is assumed but yet to be established, owing to the rarity of these tumors. They cause progressive pericardial encasement with breathlessness and chest pain; the prognosis is dire, with few surviving beyond 12 months from the time of diagnosis (15).

MDCT is superior to MRI for these tumors because the lung parenchyma and pleura can be simultaneously evaluated for signs of asbestos-related disease, i.e., calcified pleural plaques, diffuse pleural thickening, and interstitial fibrosis. Pericardial mesotheliomas appear as multiple enhancing and coalescing pericardial masses that envelop the pericardial space but rarely infiltrate deep into the underlying myocardium. As with pleural mesotheliomas, a long delay time (70–90 s) is recommended for the initial set of images because this tumor is typically poorly vascularized and may not be optimally visualized in an arterial phase study (Fig. 17).

Pericardial synovial sarcomas are extremely aggressive tumors that are composed of spindle and epithelioid cells, with imaging features that show considerable overlap with angiosarcomas. A heterogeneously enhanced multi-lobulated mass with extensive pericardial infiltration and deep invasion on MDCT has been described.

As a conclusion, MDCT can provide useful complimentary information to echocardiography and MRI for assessing a suspected cardiac mass; in some instances, it is the modality of choice for a definitive characterization. In particular, MDCT offers high spatial resolution, fast acquisition times and the

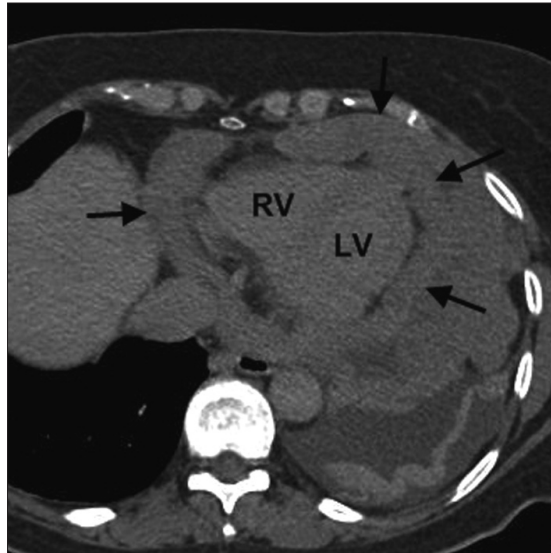


Figure 17. Pericardial mesothelioma in a patient with progressive dyspnea. This late phase (90 s) non-ECG-gated axial MDCT image shows enhancing circumferential nodular pericardial masses (arrows). RV, right ventricle; LV, left ventricle.

ability to definitively characterize fat and calcification. Radiologists should be familiar with the key distinguishing features of both neoplastic and non-neoplastic masses, as highlighted in this review.

Conflict of interest disclosure

The authors declared no conflicts of interest.

References

- Sparrow PJ, Kurian JB, Jones TR, Sivananthan MU. MR imaging of cardiac tumors. *Radiographics* 2005; 25:1255–1276.
- Syed IS, Feng D, Harris SR, et al. MR imaging of cardiac masses. *Magn Reson Imaging Clin N Am* 2008; 16:137–164.
- Hoey E, Mankad K, Puppala S, Gopalan D, Sivananthan MU. MRI and CT appearances of cardiac tumours in adults. *Clin Radiol* 2009; 12:1214–1230.
- Carbonaro, S, Villines TC, Hausleiter J, Devine PJ, Gerber TC, Taylor AJ. International, multidisciplinary update of the 2006 Appropriateness Criteria for Cardiac Computed Tomography. *J Cardiovasc Comput Tomogr* 2009; 3:224–232.
- Brodoefel H, Klumpp B, Reimann A, et al. Late myocardial enhancement assessed by 64-MSCT in reperfused porcine myocardial infarction: diagnostic accuracy of low-dose CT protocols in comparison with magnetic resonance imaging. *Eur Radiol* 2007; 17:475–483.
- Scheffel H, Baumueller S, Stolzmann P, et al. Atrial myxomas and thrombi: comparison of imaging features on CT. *AJR Am J Roentgenol* 2009; 192:639–645.
- Salanitri JC, Pereles FS. Cardiac lipoma and lipomatous hypertrophy of the interatrial septum: cardiac magnetic resonance imaging findings. *J Comput Assist Tomogr* 2004; 28:852–856.
- Grizzell JD, Ang GB. Magnetic resonance imaging of pericardial disease and cardiac masses. *Magn Reson Imaging Clin N Am* 2007; 15:579–587.
- Chiles C, Woodard PK, Gutierrez FR, Link KM. Metastatic involvement of the heart and pericardium: CT and MR imaging. *Radiographics* 2001; 21:439–449.
- Elbardissi AW, Dearani JA, Daly RC, et al. Survival after resection of primary cardiac tumors: a 48-year experience. *Circulation* 2008; 118:7–15.
- Burke A, Jeudy Jr J, Virmani R. Cardiac tumours: an update. *Heart* 2008; 94:117–123.
- Gowda RM, Khan IA, Nair CK, Mehta NJ, Vasavada BC, Sacchi TJ. Cardiac papillary fibroelastoma: comprehensive analysis of 725 cases. *Am Heart J* 2003; 146:404–410.
- Hoffmann U, Globits S, Schima W, et al. Usefulness of magnetic resonance imaging of cardiac and paracardiac masses. *Am J Cardiol* 2003; 92:890–895.
- Pigott C, Welker M, Khosla P, Higgins RS. Improved outcome with multimodality therapy in primary cardiac angiosarcoma. *Nat Clin Pract Oncol* 2008; 5:112–115.
- Kainuma S, Massai T, Yamauchi T, Takeda K, Ito H, Sawa Y. Primary malignant pericardial mesothelioma presenting as pericardial constriction. *Ann Thorac Cardiovasc Surg* 2008; 14:396–398.